Author Manuscript

Author Manuscript

Author Manuscript

Author Manuscript

HHS Public Access

Author manuscript

J Med Biol Eng. Author manuscript; available in PMC 2017 December 04.

Published in final edited form as:

J Med Biol Eng. 2017 October ; 37(5): 780–789. doi:10.1007/s40846-017-0257-x.

Pro-arrhythmogenic Effects of the V141M KCNQ1 Mutation in Short QT Syndrome and Its Potential Therapeutic Targets: Insights from Modeling

Hsiang-Chun Lee[1,2,3,4,5,6], **Yoram Rudy**[1], **Hongwu Liang**[1], **Chih-Chieh Chen**[6], **Ching-Hsing Luo**[7], **Sheng-Hsiung Sheu**[2,3,4], and **Jianmin Cui**[1]

[1]Cardiac Bioelectricity and Arrhythmia Center, Washington University in St. Louis, St. Louis, MO 63130, USA

[2]Division of Cardiology, Department of Internal Medicine, Kaohsiung Medical University Hospital, Kaohsiung Medical University, 100 Tzyou 1st Rd, Kaohsiung 807, Taiwan

[3]Faculty of Medicine, College of Medicine, Kaohsiung Medical University, Kaohsiung 807, Taiwan

[4]Center for Lipid Biosciences, Kaohsiung Medical University Hospital, Kaohsiung Medical University, Kaohsiung 807, Taiwan

[5]Lipid Science and Aging Research Center, Kaohsiung Medical University, Kaohsiung 807, Taiwan

[6]Institute of Medical Science and Technology, National Sun Yat-sen University, Kaohsiung 804, Taiwan

[7]Department of Electric Engineering, National Cheng Kung University, Tainan 804, Taiwan

Abstract

Gain-of-function mutations in the pore-forming subunit of I_{Ks} channels, KCNQ1, lead to short QT syndrome (SQTS) and lethal arrhythmias. However, how mutant I_{Ks} channels cause SQTS and the possibility of I_{Ks}-specific pharmacological treatment remain unclear. V141M KCNQ1 is a SQTS associated mutation. We studied its effect on I_{Ks} gating properties and changes in the action potentials (AP) of human ventricular myocytes. *Xenopus* oocytes were used to study the gating mechanisms of expressed V141M KCNQ1/KCNE1 channels. Computational models were used to simulate human APs in endocardial, mid-myocardial, and epicardial ventricular myocytes with and without β-adrenergic stimulation. V141M KCNQ1 caused a gain-of-function in I_{Ks} characterized by increased current density, faster activation, and slower deactivation leading to I_{Ks} accumulation. V141M KCNQ1 also caused a leftward shift of the conductance-voltage curve compared to wild type (WT) I_{Ks} ($V_{1/2}$ = 33.6 ± 4.0 mV for WT, and 24.0 ± 1.3 mV for heterozygous V141M). A Markov model of heterozygous V141M mutant I_{Ks} was developed and

Correspondence to: Sheng-Hsiung Sheu; Jianmin Cui.

Electronic supplementary material The online version of this article (doi:10.1007/s40846-017-0257-x) contains supplementary material, which is available to authorized users.

Compliance with Ethical Standards

Conflict of interest None.

Author Manuscript Author Manuscript Author Manuscript Author Manuscript

incorporated into the O'Hara–Rudy model. Compared to the WT, AP simulations demonstrated marked rate-dependent shortening of AP duration (APD) for V141M, predicting a SQTS phenotype. Transmural electrical heterogeneity was enhanced in heterozygous V141M AP simulations, especially under β-adrenergic stimulation. Computational simulations identified specific I_{K1} blockade as a beneficial pharmacologic target for reducing the transmural APD heterogeneity associated with V141M KCNQ1 mutation. V141M KCNQ1 mutation shortens ventricular APs and enhances transmural APD heterogeneity under β-adrenergic stimulation. Computational simulations identified I_{K1} blockers as a potential antiarrhythmic drug of choice for SQTS.

Keywords

Arrhythmia; Anti-arrhythmic; I_{Ks}; KCNQ1; Short QT syndrome

1 Introduction

Short QT Syndrome (SQTS) is an inherited channelopathy associated with marked shortening of QT intervals on the ECG and sudden cardiac death in individuals with structurally normal hearts [1–4]. Hereditary SQTS is genetically heterogeneous with six currently identified forms, SQT1 to SQT6, based on the chronology of their discovery [5–11]. The mutation V141M KCNQ1 causes a gain-of-function of the slow delayed rectifier potassium current (I_{Ks}) and is one of the mutations that give rise to SQT2 [12, 13].

Shortening of the QT interval is a normal physiological response to an increase in heart rate. In patients with SQTS, the QT interval is relatively normal at fast rates, but abnormally short at slow heart rates [14]. Transmural dispersion of repolarization (TDR) has been suggested to correlate to ventricular arrhythmias in an experimental SQTS model that was generated by application of an $I_{K,ATP}$ opener, pinacidil, and in patients with SQTS [15, 16]. Reducing TDR has been suggested as an important antiarrhythmic property of quinidine in a SQTS model [17] and in patients exhibiting the SQT1 variant [14]. In other forms of SQTS, data regarding pharmacological therapy remain too limited to permit specific suggestions or recommendations.

This study evaluated the effect of V141M KCNQ1 mutation on TDR and the drug effects on TDR of different anti-arrhythmic agents. First, we determined the kinetic changes relative to the wild type of V141M mutant KCNQ1 + KCNE1 channel expressed in *Xenopus* oocytes. Then we used computer simulations in the O'Hara–Rudy (ORd) human ventricular cell model to study the electrophysiological consequences of V141M KCNQ1 in ventricular myocytes in terms of its effects on I_{Ks} kinetics, action potential (AP) with and without isoproterenol (ISO) challenge, AP rate adaptation, and transmural AP duration (APD) heterogeneity. We also examined the effects of various anti-arrhythmic drugs on V141M KCNQ1-augmented transmural APD heterogeneity and identified a potential target for suppressing TDR and consequently reducing arrhythmic risk in SQT2.

Author Manuscript Author Manuscript Author Manuscript Author Manuscript

2 Methods

2.1 Mutagenesis and Oocyte Preparation

Xenopus oocytes that expressed human wild type (WT) KCNQ1 or V141M KCNQ1 and WT KCNE1 were used to record WT $I_{KCNQ1+KCNE1}$ (WT I_{Ks}) and V141M $I_{KCNQ1+KCNE1}$ (V141M I_{Ks}). KCNQ1 (provided by S. Goldstein, University of Chicago, Chicago, IL) and KCNE1 (provided by S. Nakanishi, Osaka Bioscience Institute, Osaka, Japan) were subcloned into the *Hin*dIII/*Xba*I cloning sites of pcDNA3.1+ vectors (Invitrogen, Grand Island, NY). The V141M KCNQ1 mutation was generated by using overlap extension amplification with high-fidelity polymerase chain reaction (PCR), verified by DNA sequencing (IDT technology, Coralville, IW). Messenger RNA was transcribed in vitro using the mMessage mMachine T7 polymerase kit (Applied Biosystems, Oyster Bay, NY). The follicle layer of oocytes was digested using type 1A collagenase (Sigma-Aldrich, Saint Louis, MO). Stage IV–V *Xenopus* oocytes were selected and injected with 4.6 ng mRNA per oocyte. For implementing a heterozygous genotype, we expressed heterozygous V141M I_{Ks} channels in oocytes that RNAs of WT KCNQ1 and V141M KCNQ1 at 1:1 ratio were injected. Total KCNQ1 and KCNE1 injection ratios for WT and V141M were the same at 6:1. Injected oocytes were incubated in ND96 solution (in mM: 96 NaCl, 2 KCl, 1.8 CaCl2, 1 MgCl2, and 5 Hepes, pH 7.60) at 18 °C for 3–5 days before recording.

2.2 Electrophysiology

Whole cell current recordings were obtained with the two-microelectrode voltage clamp technique. Microelectrodes were pulled from glass capillary tubes and filled with 3 M KCl. Oocytes were constantly superfused with ND96 at room temperature (~22 °C). The membrane potential was clamped using a GENECLAMP 500B amplifier (Axon Instruments, New York, NY). Data acquisition was controlled using PULSE/PULSEFIT software (HEKA, Farmingdale, NY).

2.3 Data Analysis

The electrophysiology data was analysed with Igor 4.09 (WaveMetrics, Lake Oswego, OR), and plotted with Prism 6 software (GraphPad, La Jolla, CA). Statistical evaluation was performed using the SAS program (JMP software, Version 9, Cary, NC). Where not otherwise specified, numerical variants were mean ± SD. Two-way ANOVA analysis was used, followed by Ryan-Einot-Gabriel-Welsch Multiple Range Test. A value of $p < 0.05$ was considered statistically significant.

2.4 Computational Model Simulations

Simulations of the ventricular myocyte AP were based on a modified ORd model of the human ventricular cardiomyocyte, in which the signaling cascade from ISO application to PKA phosphorylation of target proteins was incorporated [18–20]. Parameters affected by PKA phosphorylation were computed by the Heijman et al. model of the β-adrenergic signaling pathway [21]. In the simulations, 1 μmol/L ISO was applied starting from steady state after pacing at a cycle length of 1000 ms for 1000 beats. The original ORd model used data from measurements in isolated undiseased human ventricular myocytes at 37 °C to

Author Manuscript Author Manuscript Author Manuscript Author Manuscript

formulate I_{Ks} [20, 22]. In this model, the Ca^{2+} dependence of I_{Ks} was also taken into consideration. The transition rates in the I_{Ks} Markov model used here were corrected based on recordings obtained at room temperature (provided in the Supplemental Information). Simulation of I_{Ks} activation was constrained with the G–V curves and the deactivation was constrained with experimental values of Tau (see Fig. 1). The scaling factors of I_{Ks} conductance without any drug effects for Endo/Epi and Mid cells were taken from the ORd human model in which GKs for Endo and Epi were both 1.4 and for Mid was 1.0 [20].

AP durations (APD) at 95% repolarization (APD95) for endocardial (Endo), mid-myocardial (Mid), and epicardial (Epi) myocytes were measured. APD95 was measured as the interval between the time of maximum AP upstroke velocity and the time at which the membrane voltage returned to 95% of its resting value. The largest difference among Endo, Mid, and Epi APD95 was normalized by the APD95 of Mid and the value in % was used to represent TDR.

To determine how V141M KCNQ1 affects repolarization in the context of heterogeneous heart tissue, simulations were performed on a 1-dimensional transmural fiber model. The fiber was composed of 60 Epi, 45 Mid, and 60 Endo myocytes. Gap junction conductance was homogenous throughout the fiber at 1.73 μs, except for a fivefold decrease at the Mid-to-Epi transition region. A 0.5-ms current stimulus was applied to Endo cell 1 to initiate Endo-to-Epi AP propagation. The resulting conduction velocity was 44 cm/s. The QT interval on the pseudo-ECG generated by the fiber was computed as the interval between the maximum negative derivative on the QRS and the maximum positive derivative on the T-wave.

We simulated antiarrhythmic drug effects by introducing conductance changes for specific ionic currents. Using conductance scaling, Benson et al. reproduced AP changes caused by sotalol and amiodarone in canine left ventricle transmural strips [22, 23]. To simulate amiodarone application of 30–40 mg/kg/day, maximal conductance of the late sodium current (I_{NaL}) was scaled by 0.2 in Mid, and maximal conductance of I_{Ks} was scaled by 0.2 in Endo and 0.7 in Epi [23]. To simulate 100 μM/L sotalol, we scaled the rapid delayed rectifier potassium current (I_{Kr}) maximal conductance by 0.5 in Endo, 0.3 in Mid, and 0.8 in Epi [23]. To simulate 6–10 μM/L quinidine, we scaled maximal conductance of I_{NaL} by 0.6, of I_{CaL} by 0.75, of I_{Kr} by 0.6, of the inward rectifier current (I_{K1}) by 0.6 [24–26], and of the transient outward current (I_{to}) by 0.6 in Mid, by 0.46 in Endo, and by 0.6 in Epi based on experimental results from guinea-pig, rabbit, or canine ventricular myocyte studies [24–27].

3 Results

3.1 V141M Mutation Accelerates I_{Ks} Activation, Decelerates Deactivation, and Causes a Negative Shift in I_{Ks} Voltage-Dependence

The KCNQ1/KCNE1 channels that were expressed in *Xenopus* oocytes were activated every 100 s from a holding potential of −100 mV with 3 s depolarizing pulses ranging from −100 to +60 mV (Fig. 1a). We had noticed much larger instantaneous currents on shorter sweep intervals and therefore used a long sweep interval of 100 s. After each test pulse, the membrane was repolarized to −40 mV to record tail currents. Measured from the

Author Manuscript Author Manuscript Author Manuscript Author Manuscript

conductance–voltage (G–V) relation curves, heterozygous V141M KCNQ1/KCNE1 channels were activated at more negative potentials compared to the WT ($V_{1/2}$ = 33.6 ± 4.0 mV for WT, 24.0 ± 1.3 mV for V141M; n = 5 for each) (Fig. 1b). The rates of I_{Ks} activation were fitted with a double exponential function. The V141M caused faster activation of I_{Ks} at depolarizing potentials ranging from 0 to +50 mV (Fig. 1c). The same oocytes used for the voltage-dependence of I_{Ks} conductance were subjected to another pulse protocol where a depolarizing pulse was fixed at +40 mV followed by various repolarizing pulses ranging from −70 to −10 mV. The time required for tail currents to decay at different repolarizing potentials was also quantified by fitting the traces to a double exponential function. The heterozygous V141M KCNQ1 expression caused slower deactivation for I_{Ks} (Fig. 1d).

3.2 Simulated Voltage-Dependent Activation of WT I_{Ks} and Heterozygous V141M I_{Ks} is Consistent with Experimental Results

WT I_{Ks} and heterozygous V141M I_{Ks} were simulated for the voltage protocol employed in the experiment (Fig. 1a). The acceleration in I_{Ks} activation caused by the mutation was simulated by adjusting transition rates in the I_{Ks} Markov model (see Supplementary Material). The conductance-voltage relations show good agreement between the experimental and simulation results (Fig. 1b).

3.3 Simulations of Changes to Action Potentials, I_{Ks}, and I_{CaL} in Endo, Mid, and Epi Myocytes

The Markov models for WT and V141M I_{Ks} were introduced in the ORd model to simulate the AP and corresponding time course of I_{Ks} and L-type calcium current (I_{CaL}) in Endo, Mid, and Epi myocytes. Further, AP simulations were performed to evaluate the effects of β-adrenergic stimulation by using the Heijman et al. model of the β-adrenergic cascade [21] at 1 μmol/L ISO application. With V141M mutation, APD95 was shortened for all three myocyte types. The APD shortening resulted from the rapid activation of I_{Ks} and larger I_{Ks} peak amplitude during the AP (Fig. 2; Table 1). The rapidly repolarizing potential causes augmentation of I_{CaL} amplitude, especially in the presence of ISO (Fig. 2). This, in turn, resulted in a “bump” during phase-3 repolarization of the AP which was most noticeable in Mid. The magnitude of V141M-induced APD shortening was further enhanced by the presence of ISO in all three myocyte types (Table 1). Consistent with the reported clinical presentation of SQTS [28], the rate-adaptation of APD was blunted by the V141M mutation (Fig. 3).

3.4 V141M KCNQ1 Mutation Increases Transmural Heterogeneity of Repolarization

Increased transmural heterogeneity of repolarization has been suggested as a pro-arrhythmic substrate in SQTS [15]. We quantified the transmural heterogeneity of repolarization as described in the Methods section. At baseline, APD heterogeneity augmentation by the V141M mutation was most noticeable at a cycle length of 1000 ms (Fig. 3). However, in the presence of ISO, V141M-augmented APD heterogeneity was present at long and short cycle lengths as well. In WT, ISO induced less transmural APD heterogeneity at both rapid and slow cycle lengths. In contrast, with V141M KCNQ1 mutation, ISO induced more transmural heterogeneity at slow cycle lengths (Fig. 3).

Author Manuscript Author Manuscript Author Manuscript Author Manuscript

3.5 Specific I_{K1} Blockade Reduces the Transmural APD Heterogenecity

The effects of different anti-arrhythmic drug actions and several specific channel blockers on the V141M-augmented transmural APD heterogeneity were examined by computer simulations. Amiodarone and sotalol are class III antiarrhythmic agents whose main electrophysiological effects include AP prolongation [23]. However, in our simulations of the cellular effects of 100 μM/L sotalol or amiodarone (30 mg/kg/day), both drugs failed to reduce the transmural heterogeneity of APD. The next anti-arrhythmic drug we tested was quinidine, which has multiple depressing effects on sodium, calcium and potassium currents and generally prolongs the AP [24–26, 29]. Quinidine has shown promise in treating SQTS patients [30]. However, it did not reduce the transmural heterogeneity of APD in our simulations for the V141M mutation. Specific I_{Ks} blockade also failed to reduce the transmural heterogeneity of APD at either 50 or 90% blockade. Finally, with 90% specific I_{K1} blockade, the transmural heterogeneity of V141M APD was reduced below that of WT. The APD heterogeneity was reduced by specific I_{K1} blockade at both long and short cycle lengths (Fig. 4).

3.6 Specific I_{K1} Blockade Abolishes V141M Mutation-Induced QT Interval Shortening

We examined effects of the V141M KCNQ1 mutation on QT intervals of a pseudo-ECG that was computed for a 1D transmural fiber at different pacing cycle lengths (Fig. 5a). The phenotype of QT shortening was reproduced by introducing a V141M I_{Ks} Markov model into the Endo, Mid, and Epi myocytes of the fiber (Fig. 5b). The QT intervals for mutant V141M were shorter than WT at all (short and long) cycle lengths, especially with ISO challenge (Fig. 5c). V141M-induced QT shortening with ISO challenge was abolished by 90% specific I_{K1} blockade (Fig. 5b, c).

4 Discussion

The results of the present study show that: (1) the V141M KCNQ1 mutation causes gain-of-function of I_{Ks} mainly by accelerating channel activation and decelerating deactivation; (2) V141M KCNQ1 mutation-induced shortening of APs is more prominent in the presence of β-adrenergic stimulation; (3) V141M KCNQ1 augments transmural heterogeneity of repolarization, a property that has been suggested as an arrhythmogenic mechanism in SQTS; and (4) specific I_{K1} blockade has a beneficial effect of reducing the transmural APD heterogeneity and normalizing the short QT interval associated with the V141M KCNQ1 mutation.

Hong et al. reported that the V141M KCNQ1 mutation only altered the gating of I_{Ks} channels in the presence of KCNE1 auxiliary subunits [12]. They also showed that coexpression of V141M and WT KCNQ1 with KCNE1 produced a current with intermediate biophysical properties between homozygous V141M and WT I_{Ks}. Consistent with their results, our heterozygous V141M I_{Ks} also demonstrated an instantaneous current. Notably, the magnitude of the instantaneous current became smaller as we prolonged the sweep interval from 40 to 100 s. With the longer sweep interval, tail currents were suitable for an accurate fitting analysis of the G-V relationship.

Author Manuscript Author Manuscript Author Manuscript Author Manuscript

The V141M KCNQ1 mutation has been linked to SQTS2, with presentation including extremely short QT interval, fetal bradycardia, and atrial fibrillation [12, 13]. Heterogeneous AP shortening was shown to result in augmented dispersion of APD across the ventricular wall with another SQTS2 mutation [31]. Our simulations showed that the APD shortening resulting from the V141M KCNQ1 mutation is also heterogeneous (Table 1) and leads to an increase in transmural APD heterogeneity and dispersion of repolarization.

In long QT syndrome 1, which is also caused by KCNQ1 mutation affecting I_{Ks}, a greater reactivity of the sympathetic control of the QT interval has been recognized as a protective factor [32]. Similarly, it is crucial to determine the reactivity of the sympathetic control of the QT interval to evaluate the arrhythmic risk related to V141M KCNQ1 mutation. To our knowledge, there is no published report showing how the V141M mutant responds to β-adrenergic stimulation. Therefore we assumed that β-adrenergic targets are the same as in WT I_{Ks} and respond similarly to adrenergic stimulation. Based on this assumption, β-adrenergic stimulation augments APD heterogeneity for V141M KCNQ1 mutation.

In the simulations, I_{CaL} is severely reduced by including V141M in the model (Fig. 2). The literature reports a phenotype of concurrent sinus bradycardia in patients with V141M mutation [12, 13]. Reduced I_{CaL} density was shown to contribute to slowing of diastolic depolarization of the sinoatrial AP, resulting in slowing of the intrinsic heart rate, even with preserved β-adrenergic response [33]. Reduced I_{CaL} may also affect contractility, but clinical reports did not mention abnormal ventricular function [12].

Notably different from wild type, the degree of APD heterogeneity in V141M KCNQ1 is greater at a long cycle length. Reduced rate-adaptation of the QT interval has been observed in SQTS [14, 28]. SQTS2 patients with the V141M KCNQ1 mutation have been reported to present with bradycardia resulting from sinus and atrioventricular node dysfunction in utero and after birth [4, 12, 13]. Our simulations suggest that in SQTS2 with V141M KCNQ1 mutation, arrhythmia vulnerability is higher at a slow heart rate. In the simulations, both amiodarone and sotalol failed to reduce V141M-augmented APD heterogeneity. Amiodarone and sotalol can inhibit sinus and atrioventricular nodal function but can potentially worsen the bradycardia observed in SQTS2 patients. Therefore we suggest that these drugs should probably be avoided for SQTS2 patients with the V141M KCNQ1 mutation.

There has been growing evidence that quinidine is effective in treating SQTS [14, 30, 34]. However, quinidine can cause serious side effects such as thrombocytopenia and agranulocytosis [35]. In the simulations, quinidine did not reduce APD heterogeneity during β-adrenergic stimulation. An important finding of this study is that I_{K1} blockade markedly reduced APD heterogeneity in SQTS. Specific I_{K1} blockade was shown to reduce the incidence of ventricular fibrillation and ischemia–reperfusion ventricular arrhythmias in rats, rabbits, and primates by prolonging APD. Based on pioneering efforts using a transmural ventricular wedge preparation to relate the AP to electrocardiographic waveforms in experiments and in silico [36, 37], we applied the pseudo-ECG modeling approach to provide QT interval changes in KCNQ1 V141M mutation under variable conditions. The specific I_{K1} block was also effective in reducing TDR [38, 39]. Our simulations provide

Author Manuscript Author Manuscript Author Manuscript Author Manuscript

support for specific I_{K1} blockade as a potential antiarrhythmic strategy in patients with SQTS. The results are relevant to a better understanding of SQTS2, offering a clue to more feasible risk stratification, and helping to dissect the mechanisms underlying the efficacy of pharmacologic interventions.

In this study, we used the ORd model without considering the possibility of mutation effects on the membrane expression levels of I_{Ks}. In addition to affecting I_{Ks} kinetics, it is possible that the V141M KCNQ1 mutation also changes I_{Ks} densities in a transmurally heterogeneous fashion, adding to TDR. The purpose of the channel expression system is to determine the WT and V141M I_{Ks} channel kinetics in order to perform the subsequent human AP simulations. The oocyte system provide large I_{Ks} therefore the endogenous KCNQ1 current can be ignored. There are other systems would offer different advantages. The mammalian heterologous expression systems such as HEK293 cells provide feasibility for applying a physiological temperature (37 °C), and for inducing cAMP as a PKA activation. The human cardiomyocytes that are generated from inducible pluripotent stem cells would allow us to precisely determine the sensitivity to channel inhibitors or drugs for V141M mutation. However there remains problems to reproduce a homogenous population of ventricular myocytes with typical and same phenotype in dishes [40].

In conclusion, we demonstrated shortening of APD and QT in V141M KCNQ1 mutation due to accelerated activation and decelerated deactivation kinetics of I_{Ks}. The APD shortening is transmurally heterogeneous and results in increased transmural dispersion. This effect can contribute to arrhythmia vulnerability in SQTS2 patients with the V141M mutation. Simulated application of I_{K1} blocker improved transmural APD heterogeneity and QT interval widening, suggesting specific I_{K1} blockade as a potential antiarrhythmic strategy in SQTS.

Supplementary Material

Refer to Web version on PubMed Central for supplementary material.

Acknowledgments

We thank Dr. Jingyi Shi and Kelli Delaloye for KCNQ1 and KCNE1 subcloning. We thank Dr. Guohui Zhang for technical help with data analysis. We also thank Dr. Po-Yuan Chen for technical help with the computational simulation. The authors also thank the Statistical Analysis Laboratory, Department of Medical Research, Kaohsiung Medical University Hospital, Kaohsiung Medical University. This study was funded by Taiwan National Science Council Grant NSC 102-2314-B-037 -041 and KMUH97-7G31 (to HC Lee), NIH–NHLBI Grants R01-HL-049054 and R01-HL-033343 (to Y. Rudy), and NIH Grants R01-HL70393 and R01-NS060706 (to J. Cui).

References

1. Gussak I, Brugada P, Brugada J, Wright RS, Kopecky SL, Chaitman BR, et al. Idiopathic short QT interval: A new clinical syndrome? Cardiology. 2000; 94(2):99–102. [PubMed: 11173780]
2. Bjerregaard P, Gussak I. Short QT syndrome: Mechanisms, diagnosis and treatment. Nature Clinical Practice Cardiovascular Medicine. 2005; 2(2):84–87. DOI: 10.1038/ncpcardio0097
3. Schimpf R, Wolpert C, Gaita F, Giustetto C, Borggrefe M. Short QT syndrome. Cardiovascular Research. 2005; 67(3):357–366. DOI: 10.1016/j.cardiores.2005.03.026 [PubMed: 15890322]

Author Manuscript Author Manuscript Author Manuscript Author Manuscript

4. Villafañe J, Atallah J, Gollob MH, Maury P, Wolpert C, Gebauer R, et al. Long-term follow-up of a pediatric cohort with short QT syndrome. Journal of the American College of Cardiology. 2013; 61(11):1183–1191. DOI: 10.1016/j.jacc.2012.12.025 [PubMed: 23375927]
5. Brugada R, Hong K, Dumaine R, Cordeiro J, Gaita F, Borggrefe M, et al. Sudden death associated with short-QT syndrome linked to mutations in HERG. Circulation. 2004; 109(1):30–35. DOI: 10.1161/01.cir.0000109482.92774.3a [PubMed: 14676148]
6. Hong K, Bjerregaard P, Gussak I, Brugada R. Short QT syndrome and atrial fibrillation caused by mutation in KCNH2. Journal of Cardiovascular Electrophysiology. 2005; 16(4):394–396. DOI: 10.1046/j.1540-8167.2005.40621.x [PubMed: 15828882]
7. Priori SG, Pandit SV, Rivolta I, Berenfeld O, Ronchetti E, Dhamoon A, et al. A novel form of short QT syndrome (SQT3) is caused by a mutation in the KCNJ2 gene. Circulation Research. 2005; 96(7):800–807. DOI: 10.1161/01.RES.0000162101.76263.8c [PubMed: 15761194]
8. Bellocq C, van Ginneken AC, Bezzina CR, Alders M, Escande D, Mannens MM, et al. Mutation in the KCNQ1 gene leading to the short QT-interval syndrome. Circulation. 2004; 109(20):2394–2397. DOI: 10.1161/01.cir.0000130409.72142.fe [PubMed: 15159330]
9. Antzelevitch C, Pollevick GD, Cordeiro JM, Casis O, Sanguinetti MC, Aizawa Y, et al. Loss-of-function mutations in the cardiac calcium channel underlie a new clinical entity characterized by ST-segment elevation, short QT intervals, and sudden cardiac death. Circulation. 2007; 115(4):442–449. DOI: 10.1161/circulationaha.106.668392 [PubMed: 17224476]
10. Templin C, Ghadri JR, Rougier JS, Baumer A, Kaplan V, Albesa M, et al. Identification of a novel loss-of-function calcium channel gene mutation in short QT syndrome (SQTS6). European Heart Journal. 2011; 32(9):1077–1088. DOI: 10.1093/eurheartj/ehr076 [PubMed: 21383000]
11. Abriel H, Zaklyazminskaya EV. Cardiac channelopathies: Genetic and molecular mechanisms. Gene. 2013; 517(1):1–11. DOI: 10.1016/j.gene.2012.12.061 [PubMed: 23266818]
12. Hong K, Piper DR, Diaz-Valdecantos A, Brugada J, Oliva A, Burashnikov E, et al. De novo KCNQ1 mutation responsible for atrial fibrillation and short QT syndrome in utero. Cardiovascular Research. 2005; 68(3):433–440. DOI: 10.1016/j.cardiores.2005.06.023 [PubMed: 16109388]
13. Maltret A, Wiener-Vacher S, Denis C, Extramiana F, Morisseau-Durand MP, Fressart V, et al. Type 2 short QT syndrome and vestibular dysfunction: Mirror of the Jervell and Lange-Nielsen syndrome? International Journal of Cardiology. 2014; 171(2):291–293. DOI: 10.1016/j.ijcard.2013.11.078 [PubMed: 24380499]
14. Wolpert C, Schimpf R, Giustetto C, Antzelevitch C, Cordeiro J, Dumaine R, et al. Further insights into the effect of quinidine in short QT syndrome caused by a mutation in HERG. Journal of Cardiovascular Electrophysiology. 2005; 16(1):54–58. DOI: 10.1046/j.1540-8167.2005.04470.x [PubMed: 15673388]
15. Extramiana F, Antzelevitch C. Amplified transmural dispersion of repolarization as the basis for arrhythmogenesis in a canine ventricular-wedge model of short-QT syndrome. Circulation. 2004; 110(24):3661–3666. DOI: 10.1161/01.CIR.0000143078.48699.0C [PubMed: 15569843]
16. Anttonen O, Vaananen H, Junttila J, Huikuri HV, Viitasalo M. Electrocardiographic transmural dispersion of repolarization in patients with inherited short QT syndrome. Annals of Noninvasive Electrocardiology. 2008; 13(3):295–300. DOI: 10.1111/j.1542-474X.2008.00234.x [PubMed: 18713331]
17. Milberg P, Tegelkamp R, Osada N, Schimpf R, Wolpert C, Breithardt G, et al. Reduction of dispersion of repolarization and prolongation of postrepolarization refractoriness explain the antiarrhythmic effects of quinidine in a model of short QT syndrome. Journal of Cardiovascular Electrophysiology. 2007; 18(6):658–664. DOI: 10.1111/j.1540-8167.2007.00813.x [PubMed: 17521304]
18. O'Hara T, Rudy Y. Arrhythmia formation in sub-clinical ("silent") long QT syndrome requires multiple insults: Quantitative mechanistic study using the KCNQ1 mutation Q357R as example. Heart Rhythm. 2012; 9(2):275–282. DOI: 10.1016/j.hrthm.2011.09.066 [PubMed: 21952006]
19. Lee HC, Rudy Y, Po-Yuan P, Sheu SH, Chang JG, Cui J. Modulation of KCNQ1 alternative splicing regulates cardiac IKs and action potential repolarization. Heart Rhythm. 2013; 10(8): 1220–1228. DOI: 10.1016/j.hrthm.2013.04.014 [PubMed: 23608591]

Author Manuscript Author Manuscript Author Manuscript Author Manuscript

20. O'Hara T, Virág L, Varró A, Rudy Y. Simulation of the undiseased human cardiac ventricular action potential: Model formulation and experimental validation. PLoS Computational Biology. 2011; 7(5):e1002061. [PubMed: 21637795]
21. Heijman J, Volders PG, Westra RL, Rudy Y. Local control of beta-adrenergic stimulation: Effects on ventricular myocyte electrophysiology and Ca(2+)-transient. Journal of Molecular and Cellular Cardiology. 2011; 50(5):863–871. DOI: 10.1016/j.yjmcc.2011.02.007 [PubMed: 21345340]
22. Sicouri S, Moro S, Litovsky S, Elizari MV, Antzelevitch C. Chronic amiodarone reduces transmural dispersion of repolarization in the canine heart. Journal of Cardiovascular Electrophysiology. 1997; 8(11):1269–1279. [PubMed: 9395170]
23. Benson AP, Aslanidi OV, Zhang H, Holden AV. The canine virtual ventricular wall: A platform for dissecting pharmacological effects on propagation and arrhythmogenesis. Progress in Biophysics and Molecular Biology. 2008; 96(1–3):187–208. DOI: 10.1016/j.pbiomolbio.2007.08.002 [PubMed: 17915298]
24. Wu L, Guo D, Li H, Hackett J, Yan GX, Jiao Z, et al. Role of late sodium current in modulating the proarrhythmic and antiarrhythmic effects of quinidine. Heart Rhythm. 2008; 5(12):1726–1734. DOI: 10.1016/j.hrthm.2008.09.008 [PubMed: 19084812]
25. Wu MH, Su MJ, Lue HC. Age-related quinidine effects on ionic currents of rabbit cardiac myocytes. Journal of Molecular and Cellular Cardiology. 1994; 26(9):1167–1177. DOI: 10.1006/jmcc.1994.1135 [PubMed: 7529324]
26. Hiraoka M, Sawada K, Kawano S. Effects of quinidine on plateau currents of guinea-pig ventricular myocytes. Journal of Molecular and Cellular Cardiology. 1986; 18(10):1097–1106. [PubMed: 3783725]
27. Zhou P, Yang X, Li C, Gao Y, Hu D. Quinidine depresses the transmural electrical heterogeneity of transient outward potassium current of the right ventricular outflow tract free wall. Journal of Cardiovascular Disease Research. 2010; 1(1):12–18. DOI: 10.4103/0975-3583.59979 [PubMed: 21188084]
28. Patel C, Yan GX, Antzelevitch C. Short QT syndrome: From bench to bedside. Circulation: Arrhythmia and Electrophysiology. 2010; 3(4):401–408. DOI: 10.1161/circep.109.921056 [PubMed: 20716721]
29. Yatani A, Wakamori M, Mikala G, Bahinski A. Block of transient outward-type cloned cardiac K + channel currents by quinidine. Circulation Research. 1993; 73(2):351–359. [PubMed: 8330377]
30. Kaufman ES. Quinidine in short QT syndrome: An old drug for a new disease. Journal of Cardiovascular Electrophysiology. 2007; 18(6):665–666. DOI: 10.1111/j.1540-8167.2007.00815.x [PubMed: 17521305]
31. Zhang H, Kharche S, Holden AV, Hancox JC. Repolarisation and vulnerability to re-entry in the human heart with short QT syndrome arising from KCNQ1 mutation—A simulation study. Progress in Biophysics and Molecular Biology. 2008; 96(1–3):112–131. DOI: 10.1016/j.pbiomolbio.2007.07.020 [PubMed: 17905416]
32. Porta A, Girardengo G, Bari V, George AL Jr, Brink PA, Goosen A, et al. Autonomic control of heart rate and QT interval variability influences arrhythmic risk in long QT syndrome type 1. Journal of the American College of Cardiology. 2015; 65(4):367–374. DOI: 10.1016/j.jacc.2014.11.015 [PubMed: 25634836]
33. Larson ED, St Clair JR, Sumner WA, Bannister RA, Proenza C. Depressed pacemaker activity of sinoatrial node myocytes contributes to the age-dependent decline in maximum heart rate. Proceedings of the National Academy of Sciences. 2013; 110(44):18011–18016. DOI: 10.1073/pnas.1308477110
34. Gaita F, Giustetto C, Bianchi F, Schimpf R, Haissaguerre M, Calo L, et al. Short QT syndrome: Pharmacological treatment. Journal of the American College of Cardiology. 2004; 43(8):1494–1499. DOI: 10.1016/j.jacc.2004.02.034 [PubMed: 15093889]
35. Perdomo J, Yan F, Ahmadi Z, Jiang XM, Stocker R, Chong BH. Quinine-induced thrombocytopenia: Drug-dependent GPIb/IX antibodies inhibit megakaryocyte and pro-platelet production in vitro. Blood. 2011; 117(22):5975–5986. DOI: 10.1182/blood-2010-10-314310 [PubMed: 21487107]

Author Manuscript Author Manuscript Author Manuscript Author Manuscript

36. Gima K, Rudy Y. Ionic current basis of electrocardiographic waveforms: A model study. Circulation Research. 2002; 90(8):889–896. [PubMed: 11988490]

37. Antzelevitch C, Shimizu W, Yan GX, Sicouri S, Weissenburger J, Nesterenko VV, et al. The M cell: Its contribution to the ECG and to normal and abnormal electrical function of the heart. Journal of Cardiovascular Electrophysiology. 1999; 10(8):1124–1152. [PubMed: 10466495]

38. Rees SA, Curtis MJ. Further investigations into the mechanism of antifibrillatory action of the specific IK1 blocker, RP58866, assessed using the rat dual coronary perfusion model. Journal of Molecular and Cellular Cardiology. 1995; 27(12):2595–2606. DOI: 10.1006/jmcc.1995.0046 [PubMed: 8825880]

39. Rees SA, Curtis MJ. Specific IK1 blockade: A new antiarrhythmic mechanism? Effect of RP58866 on ventricular arrhythmias in rat, rabbit, and primate. Circulation. 1993; 87(6):1979–1989. [PubMed: 8504513]

40. Sinnecker D, Goedel A, Laugwitz KL, Moretti A. Induced pluripotent stem cell-derived cardiomyocytes: A versatile tool for arrhythmia research. Circulation Research. 2013; 112(6):961–968. DOI: 10.1161/circresaha.112.268623 [PubMed: 23569105]

Author Manuscript Author Manuscript Author Manuscript Author Manuscript

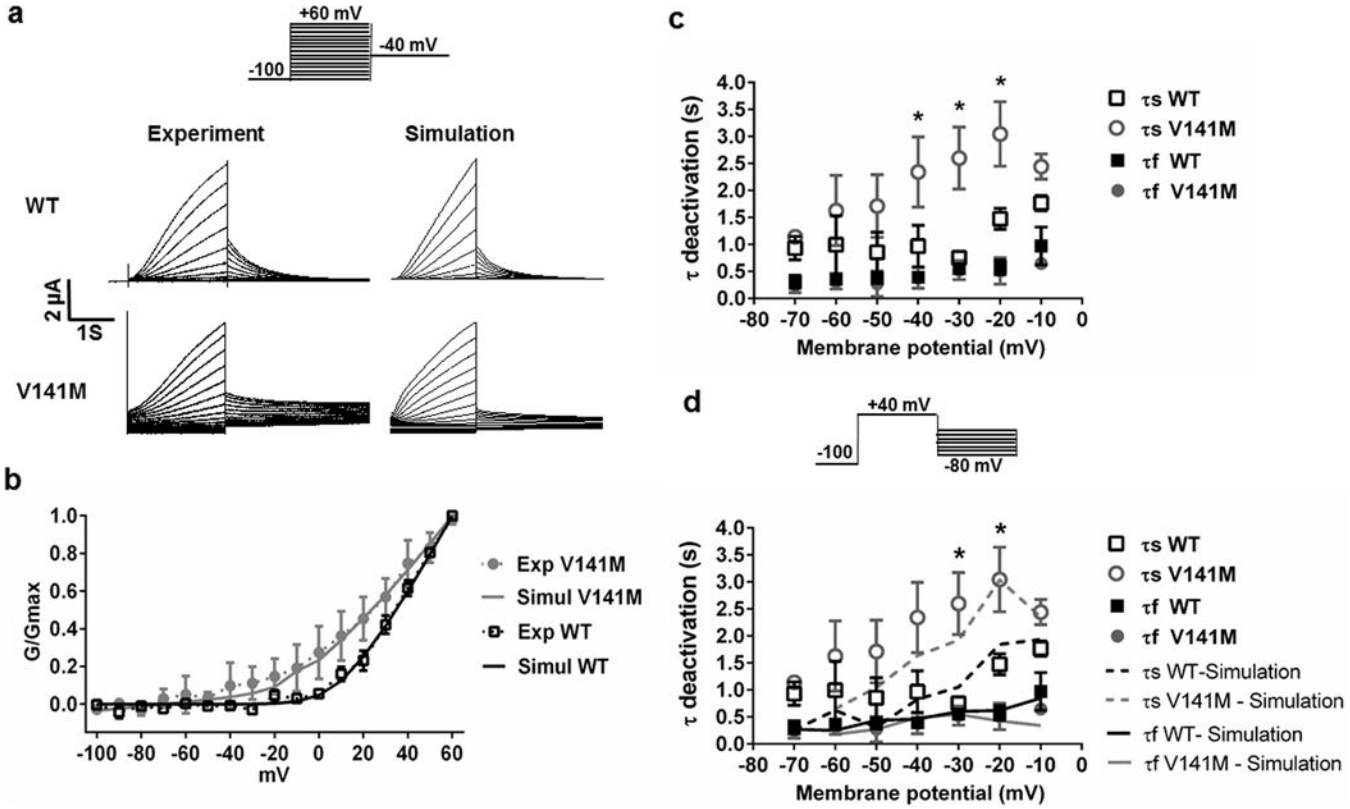

Fig. 1.

V141M KCNQ1 affects activation kinetics and voltage dependence of I_{Ks}. **a** Currents of WT KCNQ1/KCNE1 channels (WT I_{Ks}) and heterozygous V141M KCNQ1/KCNE1 channels (V141M I_{Ks}) expressed in *Xenopus* oocytes (*left panels*). The currents were elicited by test pulses to +60 mV from a holding potential of −100 mV. Tail currents were measured at −40 mV for WT and V141M I_{Ks}. The WT and V141M I_{Ks} were simulated using a Markov model (right panels; see supplementary materials). **b** V141M KCNQ1 mutation caused a leftward shift of the conductance–voltage curve ($V_{1/2}$ = 33.6 ± 4.0 mV for WT, 24.0 ± 1.3 mV for heterozygous V141M; n = 5 for each). Simulation results (*solid lines*) are consistent with the experimental data (*dashed lines*). **c** Voltage dependence of activation and deactivation time constants (**τ**) of WT and heterozygous V141M I_{Ks} (n = 5 for each). **τ** activation was obtained from fitting the activating current traces with a double exponential function. V141M KCNQ1 causes faster activation of I_{Ks} (*p < 0.05 for **τ**1 and $^{\#}$p < 0.05 for **τ**2; V141M vs WT; n = 3 for each). **d** V141M KCNQ1 causes slower deactivation of I_{Ks} (*p value <0.05 for **τ**s; V141M (n = 5) versus WT (n = 3). **τ** deactivation was obtained from fitting the deactivating current traces with a double exponential function. Lines indicate specific **τ** values for simulations

Author Manuscript Author Manuscript Author Manuscript Author Manuscript

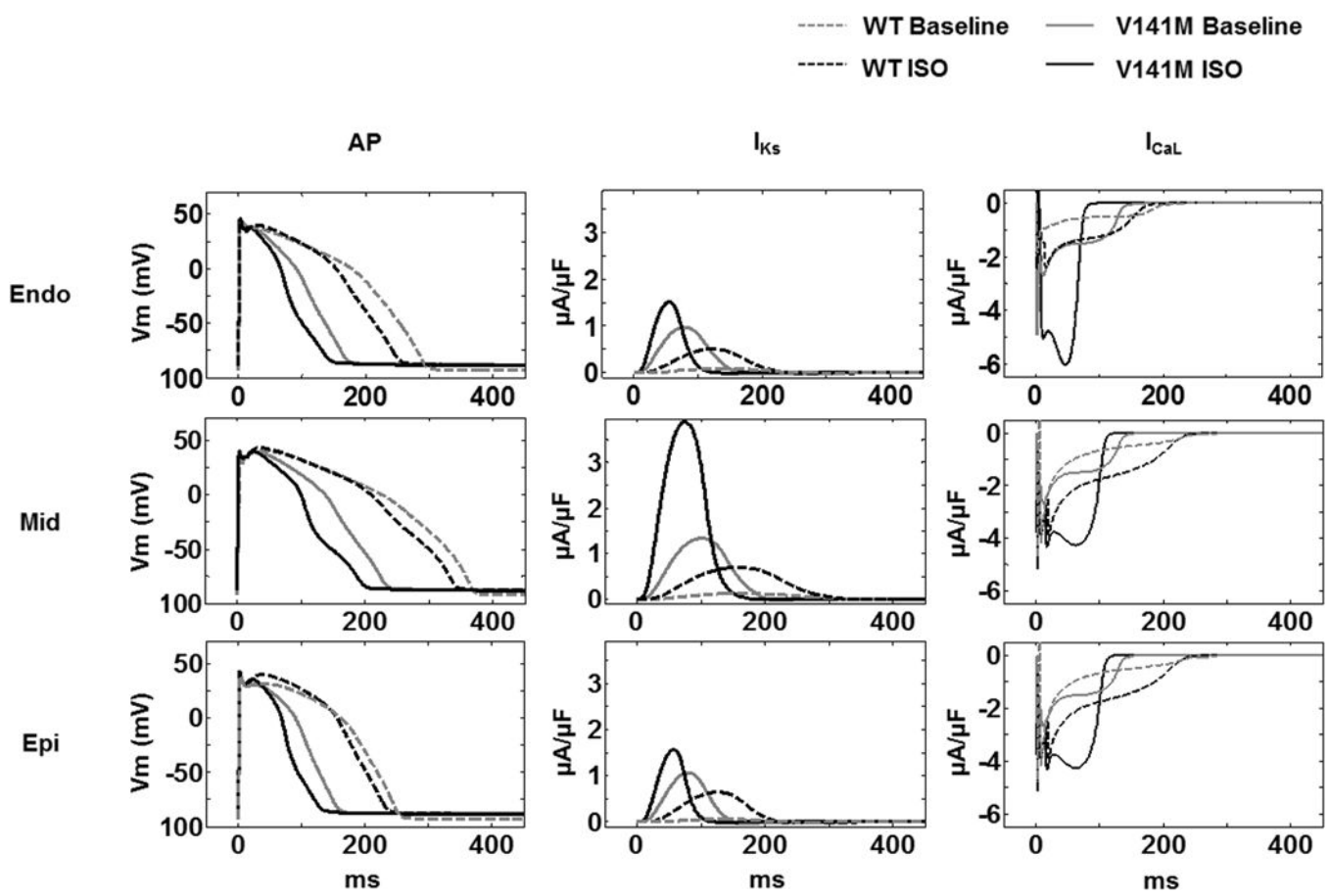

Fig. 2.

Simulated WT and heterozygous V141M KCNQ1 action potentials (AP) and the I_{Ks} and I_{CaL} during the AP in endocardial (Endo), epicardial (Epi) and midmyocardial (Mid) myocytes with and without isoproterenol (ISO). A modified O'Hara-Rudy (ORd) human ventricular myocyte model was used in the simulations. The cycle length was 1000 ms. Baseline APs (in *grey*) and APs with ISO challenge (in *black*) were simulated for WT (*dash lines*) and V141M KCNQ1 (*solid lines*) respectively. APs were shortened significantly by the V141M KCNQ1 mutation with and without ISO. In all V141M cases, I_{Ks} and I_{CaL} increased relative to WT during the AP

Author Manuscript Author Manuscript Author Manuscript Author Manuscript

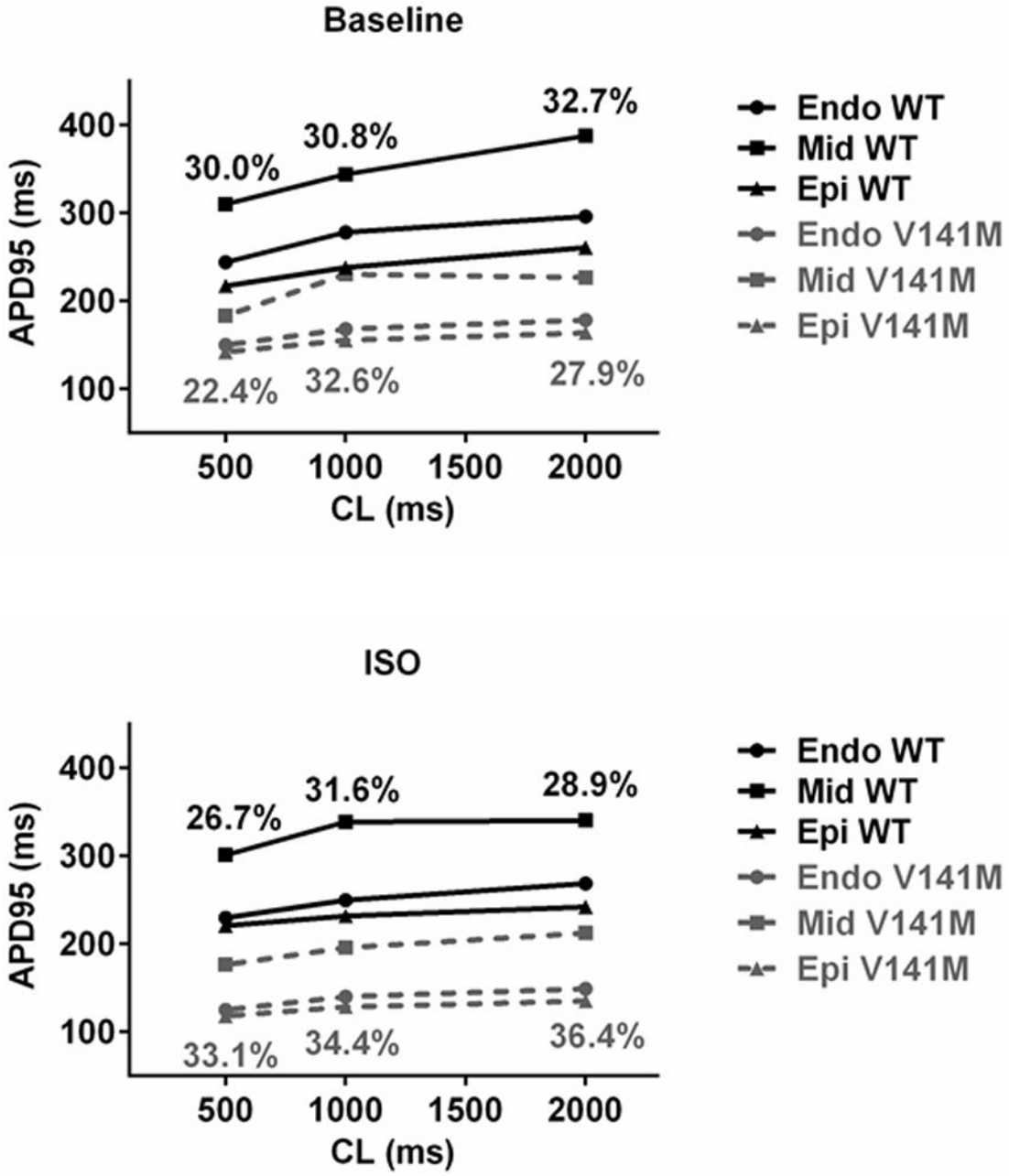

Fig. 3.

AP simulations show blunted APD rate adaptation and increased transmural heterogeneity of APD associated with the V141M KCNQ1 mutation. At fast cycle lengths of 500 ms and slow cycle lengths of 2000 ms, WT KCNQ1 APD increased 52.0, 77.6, and 43.5 ms in Endo, Mid and Epi, respectively, but V141M KCNQ1 mutation APD increased 28.3, 43.7, and 21.5 ms respectively (*upper panel*). At cycle lengths of 500 and 2000 ms, APD heterogeneity diminished from 30.0 to 26.7% and from 32.7 to 28.9% respectively in the presence of isoproterenol (ISO) challenge in WT. In contrast, the heterogeneity of APD was augmented with ISO in V141M KCNQ1. In the presence of ISO, APD heterogeneity increased from 22.4 to 33.1%, from 27.9 to 36.4%, and from 32.6 to 34.4%, at cycle lengths

Author Manuscript Author Manuscript Author Manuscript Author Manuscript

of 500, 2000, or 1000 ms, respectively. The heterogeneity increase was due to preferential abbreviation of epicardial (Epi) and endocardial (Endo) cells as compared with mid-myocardial (Mid) cells

Author Manuscript Author Manuscript Author Manuscript Author Manuscript

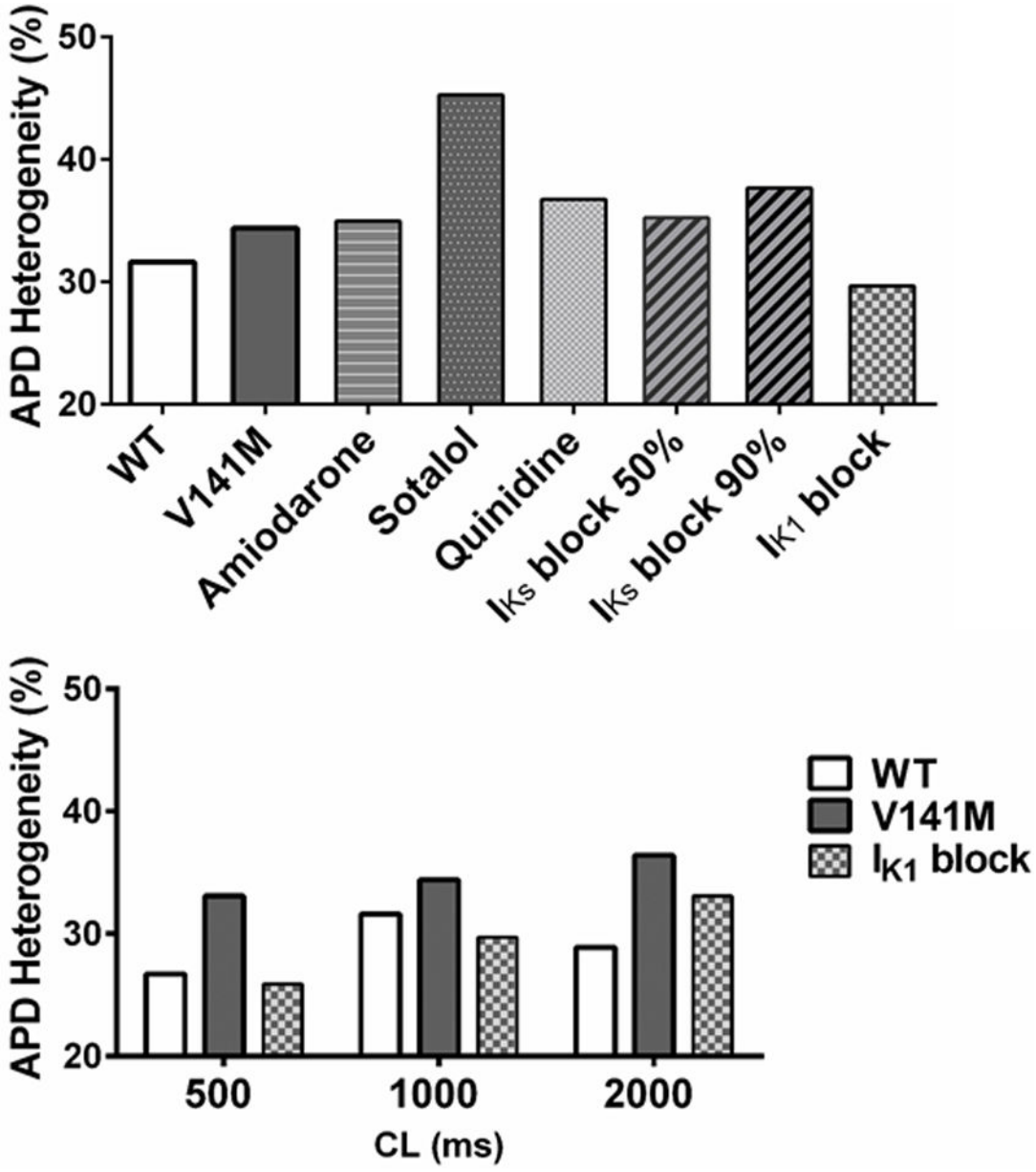

Fig. 4.

Effects of different anti-arrhythmic agents or channel blockers on the V141M KCNQ1-augmented transmural heterogeneity of APD. At a cycle length of 1000 ms with isoproterenol (ISO) (*upper panel*), amiodarone, sotalol, quinidine and I_{Ks} block (either at 50 or 90% block) all failed to reduce the mutation-augmented transmural heterogeneity of APD (*upper panel*). Only the I_{K1} block (with 90% block) improved APD heterogeneity at both long and short cycle lengths under ISO challenge (*lower panel*)

Author Manuscript Author Manuscript Author Manuscript Author Manuscript

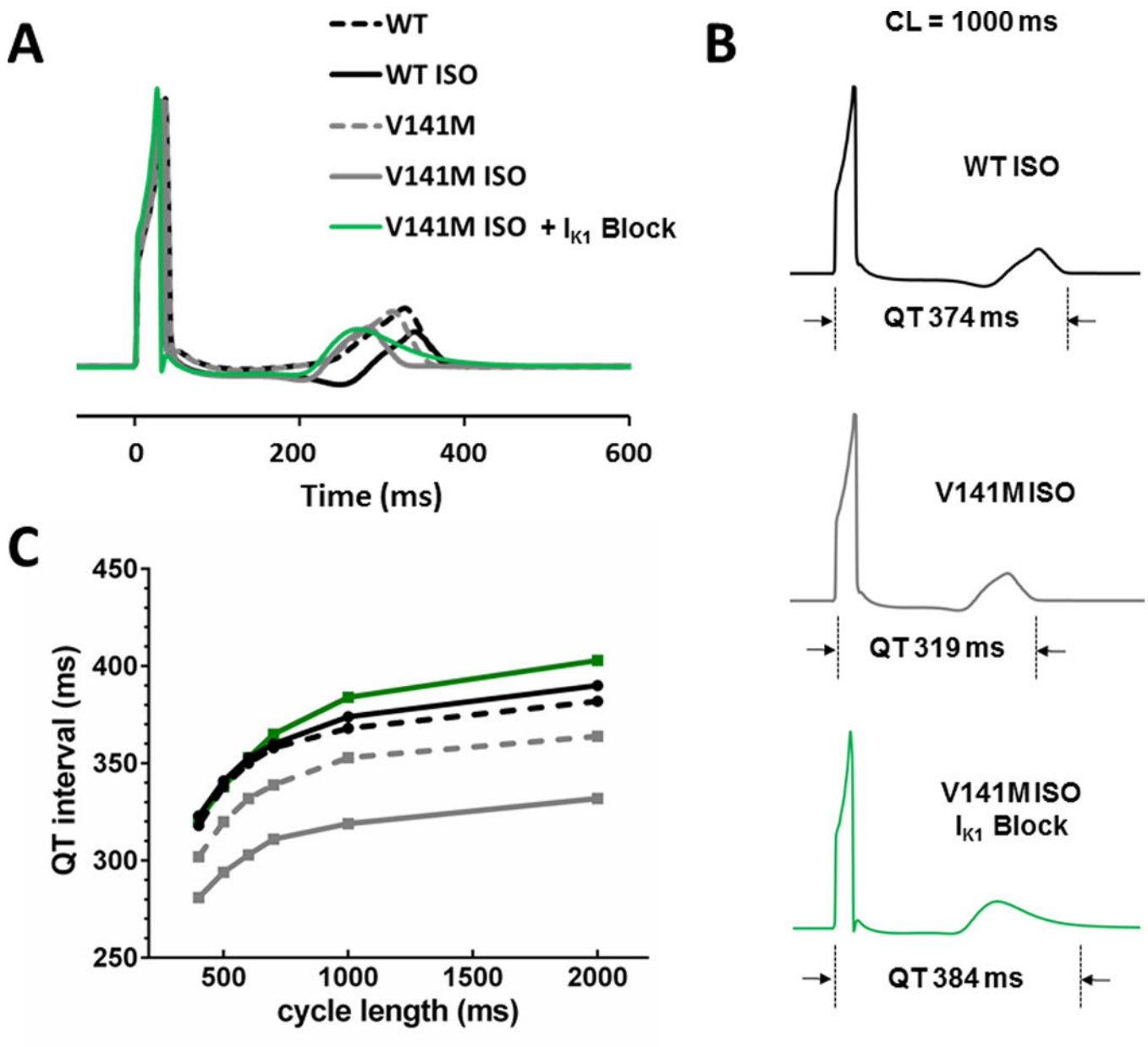

Fig. 5.

Effects of I_{K1} blockade on the pseudo-ECG and QT interval. **a** Pseudo-ECGs at a cycle length of 1000 ms for WT and V41M KCNQ1 mutation, at baseline and with isoproterenol, and with 90% I_{K1} block. **b** QT interval measurements for each pseudo-ECG are indicated. c QT intervals on the pseudo-ECG are plotted against the cycle length. In the case of V141M, the QT interval was abnormally shortened with ISO; the shortening of the QT interval was corrected by specific I_{K1} blockade. *ECG* electrocardiogram, *WT* wild type, *V141M* V141M KCNQ1 mutation

Author Manuscript Author Manuscript Author Manuscript Author Manuscript

Table 1

Computed APD_{95} and I_{Ks} for WT and V141M KCNQ1 using the ORd human ventricular model for Endo, Mid, and Epi myocytes

Myocytes	Condition	ORd human ventricular myocyte model [20]			
		APD_{95} (ms)	**Peak I_{Ks} amplitude (pA/pF)**	**APD_{95} shortening (ms/%) (V141M V.S. WT)**	**APD_{95} shortening (ms/%) (ISO V.S. baseline)**
Endo	WT	278.3	0.086		
	V141M	168.1	0.973	110.2/39.6	
	WT ISO	249.9	0.507		28.4/10.2
	V141M ISO	140.1	1.516	109.8/43.9	28.0/16.7
Mid	WT	344	0.128		
	V141M	230.6	1.336	113.4/33.0	
	WT ISO	338.9	0.696		5.1/1.5
	V141M ISO	195.7	3.898	143.2/42.3	34.9/15.1
Epi	WT	238.2	0.0695		
	V141M	155.5	1.066	82.7/34.7	
	WT ISO	231.8	0.648		6.4/2.9
	V141M ISO	128.4	1.565	103.4/44.6	27.1/17.4

Scaling factors for I_{Ks} conductance: Endo 1.4, Epi 1.4, and Mid 1.0